

## Coupled Modelling of Forest Snow Interception and Sublimation

J.W. POMEROY<sup>1</sup>, J. PARVIAINEN<sup>2</sup>, N. HEDSTROM<sup>1,2</sup>, AND D.M. GRAY<sup>2</sup>

### ABSTRACT

A series of process-based algorithms has been developed to describe the accumulation, unloading and sublimation of intercepted snow in forest canopies. These algorithms are unique in that they scale-up the physics of interception and sublimation from small-scales, where they are well-understood, to forest stand-scale calculations of intercepted snow sublimation. Evaluation of results from the set of algorithms against measured interception and sublimation in a southern boreal forest jack pine stand during late winter, found the coupled model provides reasonable approximations of both interception and sublimation losses on half-hourly, daily and event basis. Cumulative errors in estimate of intercepted snow load over 23 days of test were 0.06 mm SWE with a standard deviation of 0.46 mm SWE. Sublimation losses during the evaluation were high, approximately two-thirds of snowfall within this period. Seasonal intercepted snow sublimation as a portion of annual snowfall at the model test site was lower than sublimation during the tests, ranging from 13% for a mixed spruce-aspen, 31% for the mature pine and 40% for a mature spruce stand. The results indicate that sublimation can be a significant abstraction of water from mature evergreen stands in northern forests and that the losses can be calculated by application of process-based algorithms.

Key words: snow interception, sublimation, energy balance, boreal forest

### INTRODUCTION

High altitude and latitude forest lands are dominated by sub-alpine and boreal forests on a

global scale. These forests are primarily composed of evergreen conifer species, which retain their needles and therefore intercept snow through the winter. A survey of interception and sublimation values from North American and Russian mass balance studies (Wilm and Dunford, 1945; Miner and Trappe, 1957; Kuz'min, 1963; Troendle and Meiman, 1984; Swanson, 1986; Toews and Gluns, 1986; McNay et al., 1988; Barry, 1991) suggests that in boreal, montane and sub-alpine forests, over one-half of cumulative seasonal snowfall can remain intercepted in mid-winter, and 25% to 45% of the annual snowfall can sublimate from snow intercepted in the canopy (Pomeroy and Gray, 1995). This range has been confirmed for other snowy environments such as maritime Japan (Nakai et al., 1993). Snow interception and sublimation have been identified as important hydrological processes in high altitude and latitude forests, that as a result of particularly complex mass and energy exchanges, remain incompletely understood, though there has been recent progress in process studies (Brundl et al., 1997; Claassen and Downey, 1995; Harding and Pomeroy, 1996; Hedstrom and Pomeroy, 1998; Lundberg and Halldin, 1994; Lundberg et al., 1998; Nakai et al., 1994; Nakai et al., in press; Schmidt, 1991; Schmidt and Gluns, 1991; Schmidt et al., 1988; Pomeroy and Schmidt, 1993; Pomeroy and Gray, 1995). Lundberg and Halldin (in press) note in their comprehensive review of snow interception-sublimation studies that there has been little progress in modelling snow interception and sublimation in hydrological models. Land surface schemes of General Circulation Models (GCMs) sometimes have simple snow interception/sublimation algorithms, but these are untested and often unrealistic (Essery, 1998; Pomeroy et al., 1998).

<sup>1</sup> National Hydrology Research Centre, Environment Canada, 11 Innovation Blvd., Saskatoon, Saskatchewan S7N 3H5 Canada

<sup>2</sup> Division of Hydrology, University of Saskatchewan, Saskatoon, Saskatchewan S7N 0W0 Canada

The physically-based model of Hedstrom and Pomeroy (1998) suggests that 30 mm snow water equivalent (SWE) can be intercepted by an initially snow-free, dense, mature spruce canopy in a single snow-storm; such snow is subject to sublimation, unloading or melt. Lundberg and Halldin (1994), Harding and Pomeroy (1996) and Nakai et al. (in press) measured or estimated maximum sublimation rates from intercepted snow of 0.25-0.3 mm hr<sup>-1</sup> with a long term averages from snow-covered canopies of approximately 0.1 mm hr<sup>-1</sup>. Calculating or measuring the latent, radiative and sensible heat fluxes to intercepted snow in the canopy is considered extremely difficult because of the differing surface temperature, albedo and roughness of intercepted snow and the surrounding evergreen canopy and because of difficult to quantify heat storage terms in the canopy and micro-scale advection of energy between canopy and snow (Harding and Pomeroy, 1996). At larger scales, the strong energy balance divergence between snow-covered surfaces and snow-free evergreen forest canopies induces advective flows of energy that make calculations of aggregated mass and energy exchange extremely complex (Taylor et al., 1998). Many researchers have applied Penman-Monteith-style combination equations to calculate mass and energy exchange with intercepted snow (Lundberg and Halldin, 1994; Nakai et al., 1994). The models use a canopy-scale energy balance and parameterise the energy and mass exchanges occurring within the canopy with variable aerodynamic resistances to empirically account for changing snow surface area, location of snow within the canopy, penetration of wind within the canopy, conductive heat exchange and radiative heat exchange between canopy and snow. The models do not generally account for heat storage by the canopy.

This paper proceeds from the premise that our understanding and description of complex phenomenon at large scales is enhanced from an appreciation of the physical processes and application of the continuity equation at immediately smaller scales. It is therefore the objective of this paper to outline and demonstrate a physically-based, multi-scale energy balance model of coupled snow interception and sublimation. The model is unique in that it takes the physical understanding of snow interception from the branch-scale and applies this to the canopy, and then takes the corresponding understanding of snow sublimation of a single snow particle and applies this to intercepted snow in the canopy. The model results are compared to field measurements and placed in the context of seasonal snow interception and sublimation from a boreal forest.

## THEORY

As a step towards more fully understanding the multi-scale energy fluxes that control sublimation rates, the theory of intercepted snow sublimation is presented as an energy and mass balance at a small-scale and then scaled up to the canopy. Scaling is accomplished using the following equation, which multiplies a sublimation rate coefficient for intercepted snow in the canopy,  $V_i$  (s<sup>-1</sup>) calculated from a particle-scale mass and energy balance, adjusted for the exposure of intercepted snow in the canopy, with the intercepted snow mass per unit area of ground,  $I$  (kg m<sup>-2</sup>) to find the sublimation flux,  $q_s$  (kg m<sup>-2</sup> s<sup>-1</sup>)

$$q_s = V_i I \quad (1)$$

### *Sublimation rate for an ice sphere*

Schmidt (1991) examined intercepted snow surface structure and noted its similarity to a collection of tiny ice particles. If the reader is unable to do so on an excursion to a snowy forest, they can make similar observations from Fig. 1. Schmidt then adapted a sublimation model that had been used for blowing snow particles (Thorpe and Mason, 1966; Schmidt, 1972; Pomeroy, 1989) to calculate intercepted snow sublimation.

The assumption of an equilibrium between the latent heat associated with convective and radiative heat transfer to a snow particle and the diffusive and convective transport of water vapour from the particle permits the development of a "thermodynamic



*Figure 1. Close-up photograph of intercepted snow found near Waskesiu Lake, Saskatchewan, showing crystal fragment projections and small-scale irregularities.*

equilibrium" sublimation model (Thorpe and Mason, 1966; Schmidt, 1972; 1991; Pomeroy et al., 1993; Pomeroy and Gray, 1995). The rate that water vapour mass,  $m$ , can be removed,  $dm/dt$ , from an ice particle of radius,  $r$ , depends on the water vapour density difference ( $\rho_{wa} - \rho_{wp}$ ), where  $\rho_{wa}$  is the density in the remote environment and  $\rho_{wp}$  is the density at the particle surface. If  $D$  is the diffusivity of water vapour in still air, and  $Sh$  is the Sherwood Number, indexing the turbulent transfer of water vapour, then

$$\frac{dm}{dt} = 2 \pi r D Sh (\rho_{wa} - \rho_{wp}) \quad (2)$$

Convection of heat to or from the particle provides the energy necessary for the mass flux,

$$h_s \left( \frac{dm}{dt} \right) = 2 \pi r \lambda_T Nu (T_p - T_a) \quad (3)$$

where  $h_s$  is the latent heat of sublimation,  $\lambda_T$  is the thermal conductivity of air,  $Nu$  is the Nusselt Number, indexing turbulent transfer of sensible heat,  $T_a$  is the ambient air temperature,  $T_p$  is the temperature at the ice particle surface. Lee (1975) derived the relationship between the dimensionless Nusselt and Sherwood Numbers and the particle Reynolds Number,  $N_R$ , for  $0 < N_R < 10$  as,

$$Nu = Sh = 1.79 + 0.606 N_R^{0.5} \quad (4)$$

where  $N_R = 2rV/\nu$  with ventilation speed,  $V$ , and kinematic viscosity of air,  $\nu$ .

Thorpe and Mason (1966) presumed that snow particles remain in thermodynamic equilibrium with a surface temperature at the "ice bulb" temperature and water vapour density at the particle surface saturated with respect to ice and the ambient air temperature. They then demonstrated the use of the Clausius-Clapeyron equation to combine Eqs. 2 and 3. Schmidt (1972) added shortwave radiative heat transfer to the energy balance formulation, presuming that net longwave fluxes were small. These developments provide the physically-based energy balance equation for sublimation of an ice sphere that is suitable for implementation in calculating a sublimation rate coefficient for single ice spheres,  $V_s$  ( $s^{-1}$ ), where

$$V_s = \frac{dm}{m dt} = \frac{2 \pi r (\rho_{wa} - \rho_s) - S^* J}{h_s J + \frac{1}{D \rho_s Sh}} \quad (5)$$

and  $\rho_s$  is the saturation water vapour density at temperature  $T_s$ .  $J$  is found as,

$$J = \frac{1}{\lambda_T T_a Nu} \left[ \frac{h_s M}{R T_a} - 1 \right] \quad (6)$$

where  $R$  is the universal gas constant and  $M$  is the molecular weight of water.  $S^*$  is the net shortwave radiation flux to the particle, found as

$$S^* = \pi r^2 (1 - \alpha) S \downarrow \quad (7)$$

where  $\alpha$  is particle shortwave albedo and  $S \downarrow$  is the incoming shortwave radiation. Values of constants and coefficients for use in applying Eqs. 5 - 7 are compiled by Pomeroy and Gray (1995). The calculation is evaluated and demonstrated for intercepted snow by Schmidt (1991), using an additional scaling factor that accounted for the shape of snow on an artificial tree.

#### Exposure coefficient

Snow intercepted on branches in the canopy is not as well-exposed to the atmosphere as a single isolated ice sphere, as many ice spheres are contained within intercepted snow masses. For a canopy subject to uniform micrometeorological conditions, the sublimation rate coefficient must be modified to account for the deviation in actual exposure of snow to that of an ideal ice sphere. This is simply specified as,

$$V_I = V_s C_e \quad (8)$$

where  $V_I$  is the sublimation rate coefficient for snow in the canopy and  $C_e$  is a dimensionless exposure coefficient (Pomeroy and Schmidt, 1993). Pomeroy and Schmidt (1993) provided a geometric definition of  $C_e$  as the surface area ( $A_I$ ) to mass ( $I$ ) ratio of intercepted snow divided by the surface area ( $A_m$ ) to mass ( $m$ ) ratio of a single ice sphere, where,

$$C_e = \frac{m A_I}{I A_m} \quad (9)$$

The surface area of intercepted snow is extremely difficult to directly measure due to its three dimensional structure, requiring that another method be used to find  $C_e$ .

By Eq. 8,  $C_e$  can be found from the ratio of intercepted snow to ice sphere sublimation rate coefficients, where,

$$C_e = \frac{m \frac{dI}{dt}}{I \frac{dm}{dt}} \quad (10)$$

For convenience,  $m$  is specified as the mass of a 500  $\mu\text{m}$  radius ice sphere with a density of  $1000 \text{ kg m}^{-3}$ . Pomeroy and Schmidt (1993) related  $C_e$ , calculated in this manner to Schmidt's (1991) measurements of sublimation rate from snow intercepted on an artificial evergreen (commercial "Christmas tree", Schmidt et al., 1988), calculations of sublimation rate for an ideal ice sphere (as specified above) and expression for sublimation rate of snow on an artificial evergreen to that for an ice sphere. The resulting expression is

$$C_e = k \left(\frac{I}{I^*}\right)^{-F} \quad (11)$$

where  $k$  is a dimensionless coefficient indexing the shape of snow (found to be 0.00011 for fresh and 0.000055 for old snow on the artificial evergreen),  $I^*$  is the maximum intercepted snow load for the canopy (or tree in Schmidt's case) and  $F$  is an exponent having a value of 0.3 for snow on the artificial tree. It is presumed that older intercepted snow becomes simplified in its shape, as small, isolated masses of snow are better-exposed than large masses and hence likely to sublimate more quickly. Equation 11 specifies that the exposure coefficient decreases as intercepted snow load increases and as intercepted snow ages. The relationship is derived from an artificial evergreen that is much smaller and different in form than natural conifers, and thus its extrapolation to a natural coniferous forest requires a method to quantify the mass, sublimation rate and surface area of intercepted snow in natural canopies in order to test the values of  $k$  and  $F$  (Pomeroy and Schmidt, 1993).

#### Fractal geometry of intercepted snow

An alternative to physical measurements of sublimation rates to determine  $C_e$  is the use of fractal analysis. Natural objects, such as forest canopy shapes and melting snow patches (Mandelbrot, 1983; Shook et al., 1993), can often be described by fractal

geometry over a range of scales for which they "behave" as fractals, and simple recursive fractal algorithms can create objects strongly resembling conifers and snow crystals. These objects suggest that the volume and surface area of intercepted snow can be described mathematically by fractal geometry.

One measure commonly used in fractal mathematics to evaluate the degree of irregularity of an object is its dimension  $D$ . Euclidean objects have integer values for  $D$ . For example, the perimeter of circles and squares have a  $D$  of 1 and the surface area of spheres and cubes have a  $D$  of 2, whereas a more convoluted object will have values of  $D$  larger than that of Euclidean objects. The  $D$  of fractal objects can be broken down into Euclidean and fractal components. For example, to find the dimension of a fractal perimeter  $D$ , of a plane slice through a volume, the Euclidean component ( $D_e$ ) = 1 is added to the fractal component ( $D_f$ ),

$$D = D_e + D_f \quad (12)$$

If the object is self similar in all directions, then the dimension of the fractal surface area can be found by increasing the Euclidean component to 2 and adding the same fractal component (Pomeroy and Schmidt, 1993). If snow on trees is self similar in all directions, then the perimeter and cross sectional areas of intercepted snow can be useful in determining the dimension of the surface area of intercepted snow, and hence the relationship between surface area and volume (and therefore mass). This is because the dimension,  $D$ , of a collection of perimeters,  $P$ , of objects that are fractal, can be found empirically from their individual areas,  $A$ , by the expression (Mandelbrot, 1983),

$$P = k_1 A^{\frac{D}{2}} \quad (13)$$

where  $k_1$  is a scale coefficient whose magnitude depends on the scale of measurement of  $P$  and  $A$ . Experimental results by Pomeroy and Schmidt (1993) demonstrate that intercepted snow is indeed self similar, and that such a method is viable.

Pomeroy and Schmidt (1993) used a combination of dimensional analysis and fractal mathematics to evaluate the exposure coefficient. Substituting volume ( $V$ ) and density ( $\rho$ ) for mass in Eq. 9, assuming that the ice sphere is Euclidean ( $D = D_e$ ) in its surface area and volume, and the canopy snow is similarly fractal ( $D = D_e + D_f$ ) in all dimensions of its surface area and volume, the equation becomes

$$C_e = \frac{A_f V_E \rho}{A_E V_f \rho} = \frac{L_E}{L_f} = \frac{L^1}{L^{(1+D_f)}} = L^{-D_f} = L^{(1-D)} \quad (14)$$

where A = area, L = length and the subscripts f and E refer to fractal and Euclidean objects respectively. reducing to a Euclidean length over a fractal length, therefore having dimensions of  $-D_f$ . Because  $I/I^*$  and k in Eq. 9 are dimensionless, then  $D_f = F$ .  $D_f$  can be found empirically from Eq. 13 as  $D-1$  (Pomeroy and Schmidt, 1993).

Experimental results of Pomeroy and Schmidt (1993) from boreal forest evergreen photographs show that the fractal dimension  $D_f$  of intercepted snow for individual branches on the lower canopy of a natural spruce stand was centred about 0.3, identical to that of the exponent F of Eq. 11 for sublimation data from Schmidt's (1991) artificial spruce tree. In the upper canopy, F increased to approximately 0.37 or higher. The results suggested that geometric analysis of photographs of intercepted snow can determine the coefficient, F in Eq. 11.

### Intercepted Snow Mass

It is necessary to know the intercepted snow mass I to calculate sublimation rate in Eq. 1, and the maximum snow load,  $I^*$ , to calculate the exposure coefficient in Eq. 11. Hedstrom and Pomeroy (1998) presented a process-based model of intercepted snow accumulation which permits the calculation of both from standard meteorological parameters, the existing load of intercepted snow and forest stand descriptors. The model can be summarised as,

$$I = I_1 e^{-U t}, \quad I_1 = (I^* - L_o) \left(1 - e^{-\frac{c_p P}{I^*}}\right) \quad (15)$$

where  $I_1$  is snow interception before unloading,  $L_o$  is the initial intercepted snow load, P is snowfall,  $c_p$  is the "canopy-leaf contact area per unit area of ground" which for no wind is the proportional canopy coverage and in high wind speeds is 1, U is a snow unloading coefficient and t is time since the previous snowfall. The maximum canopy snow load (maximum interception),  $I^*$ , is found using winter leaf area index (LAI) and maximum canopy load, estimated using a procedure developed by Schmidt and Gluns (1991), as:

$$I^* = \bar{S} \left(0.27 + \frac{46}{\rho_s}\right) LAI \quad (16)$$

where  $\bar{S}$  is the mean maximum snow load per unit area of a branch ( $\text{kg m}^{-2}$ ), corrected using,  $\rho_s$ , the

density of fresh snowfall ( $\text{kg m}^{-3}$ ). Hedstrom and Pomeroy (1998) could not find a method to calculate U from first principles and suggested a value for  $e^{-Ut}$  of 0.678 from weekly tests over four years. For modelling coupled interception and sublimation on short time steps, a reasonable modification of the interception model is to use  $I_1$  rather than I for sublimation calculations, as sublimation proceeds immediately and unloading proceeds with increasing probability as time increases. After sublimation had depleted  $I_1$ , it would be substituted into Eq. 15 and unloading calculated as a proportion of the depleted interception. The resulting sublimated and unloaded I would then be declared  $L_o$  for the next time step calculation.

## METHODOLOGY

### Site

The primary site is a level jack pine stand in the southern boreal forest of central Canada (Waskesiu Lake, Prince Albert National Park, Saskatchewan). Waskesiu Lake is cool and sub-humid with 6-7 months of snow cover and a cold dry winter. The pine stand is composed of mature trees 16-22 m tall with a sparse understorey of deciduous bushes. Leaf area index (LAIW) in winter is  $2.2 \text{ m}^2 \text{ m}^{-2}$  and canopy coverage is 82% as measured with a LICOR LAI-2000 (Gower and Norman, 1991). Other sites referred to are a mature black spruce stand (LAIW= $4.1 \text{ m}^2 \text{ m}^{-2}$ ) and a mature mixed-wood (white spruce and trembling aspen) stand (LAIW=0.7); both stands are located within a few km of the pine. A digital photograph of snow in the pine canopy (Fig. 2),

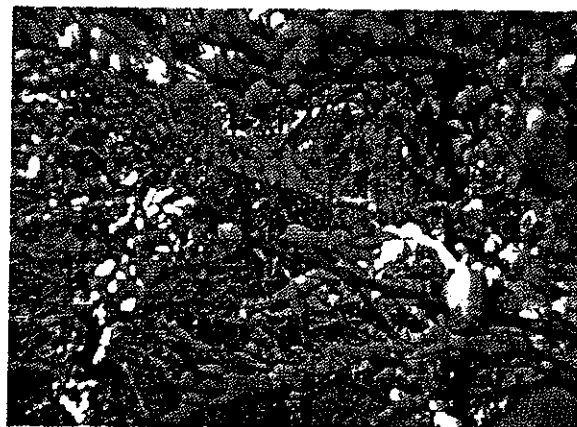


Figure 2. Digital photograph of intercepted snow in the jack pine canopy near Waskesiu Lake, Saskatchewan. Note that the snow is well-exposed to the atmosphere as it is dispersed throughout the canopy. This type of digital photograph was analysed to calculate the fractal dimension of intercepted snow.

provides an example of the images analysed for fractal dimension and an impression of canopy structure and snow load. Other studies conducted here further describe the site, local climate and canopy characteristics (Harding and Pomeroy, 1996; Pomeroy and Dion, 1996; Pomeroy et al., 1997; Hedstrom and Pomeroy, 1998).

### Instrumentation

Instrumentation included a "Radiation and Energy Balance Systems" net radiometer and upward and downward facing "Kipp and Zonen" solarimeters (pyranometers) at a height of 27 metres, measuring radiative fluxes above the canopy; upward and downward facing "Delta-T" tube solarimeters and a "Delta-T" 1-metre long tube net radiometer at a height of one metre, measuring radiative fluxes below the canopy; "Vaisala" HMP35CF hygrometers in "Gill" radiation shields at 12 and 20 m heights, measuring air temperature and humidity; two "RM Young" vertical anemometers and two "RM Young" directional anemometers at heights of 12 and 20 metres, measuring vertical wind speed and horizontal wind speed and direction within the canopy, respectively. University of Saskatchewan optoelectronic Snow Particle Detectors (Brown and Pomeroy, 1989) were used to record times and relative rates of snowfall above and below the canopy and to help detect unloading of intercepted snow. This equipment sampled meteorological parameters once per minute, with average values and wind statistics recorded each 30 min. Campbell 21X and CR10 microloggers controlled instrumentation and digitised and retrieved data.

A "Logitech Fotoman" digital camera was mounted in an insulated and heated protective enclosure at a height of 12 metres, recording oblique digital images of canopy intercepted snow at Noon each day. The camera stores 256 level gray-scale images with a resolution of 496x360 pixels. The weight of intercepted snow on a single, full-size tree was measured by cutting, sealing the base with tar and freely-suspending a local tree from a "T-Hydrionics" force transducer (Pomeroy and Schmidt, 1993; Hedstrom and Pomeroy, 1998). The force transducer was temperature compensated and repeated tests with known weights were used to develop an empirical temperature correction equation, reducing errors to less than 50 g out of up to 20 kg of snow load.

Nipher-shielded Atmospheric Environment Service snowfall cylinders were installed under each canopy and in a small clearing nearby. These cylinders were emptied and measured weekly. At the same time a survey of snowcover depth and density

using an ESC-30 snow density gauge was conducted along assigned 10-point lines under each canopy type.

### Data Analysis

As described by Hedstrom and Pomeroy (1998), sub-canopy snowfall was determined by comparing weekly snowfall at the Nipher-shielded gauge to increases in snow accumulation for weeks in which no melt occurred, and deriving a correction factor to scale from the point gauge measurement to the stand. Snowfall rates were calculated for half-hourly periods by comparing total snow particle counts each week to the weekly snowfall and assigning a mean particle mass. Seasonal sublimation for each stand type was estimated as the difference between cumulative above- and corrected sub-canopy snowfall at a time when no snow was observed to remain in the canopy (end of winter).

The mass of intercepted snow on the tree was converted to an areal snow water equivalent (SWE mm) using the technique described by Hedstrom and Pomeroy (1998) where the tree snow mass is multiplied by a scaling parameter equal to the mean ratio of increases in mass on the tree to the difference in above- and adjusted below-canopy snowfall. Sublimation or interception rates were calculated by the change in snow mass on the tree, scaled-up to a change in canopy snow mass per unit area as described above. Snowfall occurrence was used to identify periods of "pure" sublimation and mixed interception/sublimation.

Periods were selected for sublimation analysis based on the following criteria: i) clean radiometers, working instrumentation and frequent manned observations, ii) no snowfall, iii) no apparent unloading or wind redistribution of snow, iv) no evidence of intercepted snow melt, iii) no rainfall, iv) clear sublimation sequences with a continuous loss of intercepted mass. For coupled sublimation/interception analyses, periods with snowfall and unloading were included.

Water vapour densities were calculated with respect to ice from air temperature and relative humidity measurements at a height of 12 m (centred on canopy leaves). Snow ventilation speed was measured at 12 and 18 m height and found as the sum of horizontal wind speed, mean vertical wind speed and the half-hourly variance of the vertical wind speed. Net solar radiation for the ice sphere was calculated using incoming solar radiation at the canopy top and an assumed particle albedo of 0.8.

Fractal dimension of intercepted snow was determined by perimeters and areas of digitised oblique photographs of intercepted snow with the programme "Mocha" by Jandel Scientific as described

by Pomeroy and Schmidt (1993). Each image normally contained thousands of snow objects. The log-log slope of the relationship between perimeters and areas of these objects provided  $D/2$ . The fit of Eq. 13 was normally excellent with  $r^2 > 0.98$  as found by Pomeroy and Schmidt (1993), confirming that intercepted snow behaved sufficiently as a fractal object for the purposes of analysis.

### Model Implementation

Measured data provided the following parameters, which are used to run the model: ventilation speed, ambient air temperature, water vapour density, incoming shortwave radiation, intercepted snow fractal dimension, snowfall. The model calculates variables in the following sequence for each half-hour: i) interception (without unloading parameter  $e^{-U_t}$ ), ii) sublimation, iii) unloading ( $e^{-U_t}$  multiplied by the remaining intercepted mass after sublimation). The measured parameters used to evaluate the model are intercepted snow mass, intercepted snow sublimation rate, episodic/seasonal sublimation, episodic interception.

### Fractal Dimension

To determine  $F$  for the pine canopy, 93 daily photographs of canopy snow were analysed for perimeter to area relationships over the winters of 1994-95 and 1995-96 using Eq. 13. The daily  $F$  values were compared to time since fresh snowfall, air temperature and intercepted snow load to determine if the fractal dimension of intercepted snow could be predicted as a function of interception loading or degree of sublimation (Fig. 3). As shown in Fig. 3,  $F$  ranged from 0.33 to 0.43 and showed no trend with snow age, air temperature or snow load, though the scatter in  $F$  values diminished as snow load increased. The average  $F$  over two years of measurement was 0.4. The similarity of the  $F$  values measured here for pine canopies to those measured by Pomeroy and Schmidt (1993) for a black spruce canopy suggests the value of 0.4 might be widely applicable and an intrinsic feature of snow intercepted on evergreens.

### Snow Shape Coefficient

No method exists to directly measure the snow shape coefficient,  $k$ . To calculate  $k$  indirectly, Eqs. 1, 8 and 11 were re-arranged to solve for  $k$ .  $k$  was calculated for 152 half-hourly periods in 1995, using the intercepted snow sublimation rate,  $q_e$ , and intercepted snow mass,  $I$ , from the weighed tree; the sublimation rate coefficient for a 500  $\mu\text{m}$  radius ice sphere,  $V_s$ , from measured meteorological parameters; maximum intercepted snow load,  $I^*$ , from leaf area index, snow density and species type and  $F$ , which

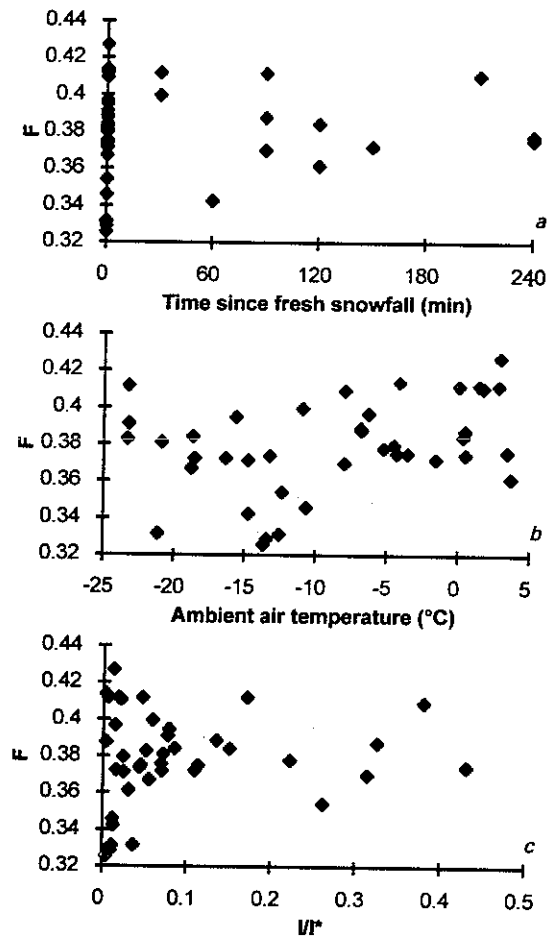


Figure 3. Relationship between measured fractal dimension,  $F$ , and a) snow age, b) air temperature, c) relative interception  $I/I^*$  (interception/maximum interception) for 1995 data. Trends for 1996 were similar.

was set to 0.4 as described above. The resulting values for  $k$  (Fig. 4) are substantially higher than those Pomeroy and Schmidt (1993) determined from Schmidt's (1991) measurements from an artificial evergreen (0.00005 to 0.0001); the difference could be due to several factors including: i) better exposure of snow in a natural mature pine canopy compared to a small artificial spruce, ii) ventilation of snow particles within intercepted snow clumps as proposed by Claassen and Downey (1995) or iii) underestimation of the energy inputs to intercepted snow in the model. No clear trend between  $k$  and time since fresh snowfall, ambient air temperature or intercepted snow load could be found, though in agreement with the theory of Pomeroy and Schmidt, older snow had generally lower  $k$  values as did higher snow loads. For the purposes of modelling,  $k$  was set to its average value of 0.0114.

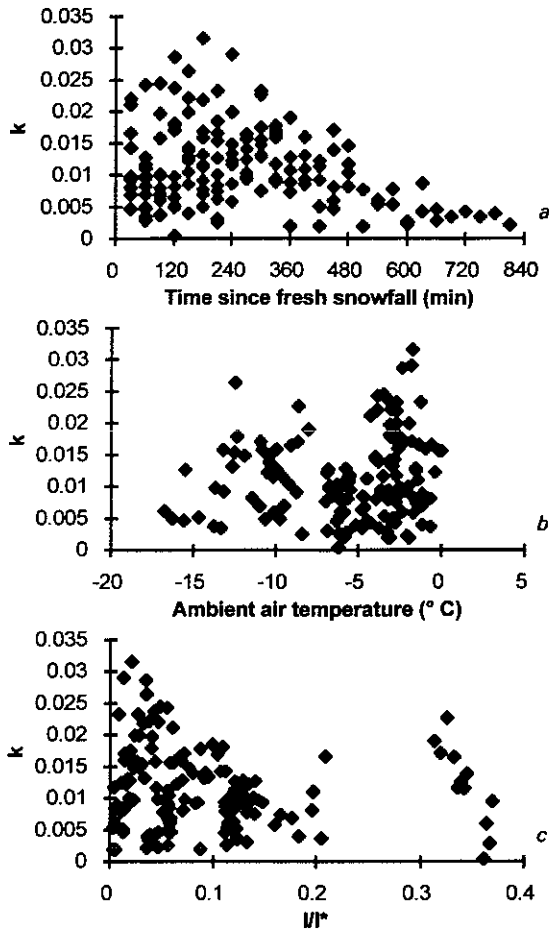


Figure 4. Relationship between snow shape factor,  $k$ , and a) snow age, b) air temperature, and c) relative interception,  $II^*$  (interception/maximum interception) for 1995 data.

## MEASUREMENT AND MODEL RESULTS

(Feb/Mar) in 1995 and 1996 were selected for analysis. 1995 was the cooler year with three events of

5-10 days whilst 1996 had four events of 1-4 day lengths. Dates and meteorological conditions for sublimation are shown in Table 1 and are typical of late winter in the southern boreal forest.

### Sublimation Model

To evaluate the sublimation model in isolation from the interception model, the modelled cumulative sublimation over each event was compared to the measured loss of snow mass from the weighed tree - converted to mm SWE and shown in Fig. 5. The events ranged from 1.5 to 4.8 mm SWE of sublimation loss. The sublimation model was run by providing the measured intercepted load at the beginning of the event and letting the model calculate sublimation until this load was depleted. It is assumed that loss of mass of snow from the tree is completely due to sublimation, an assumption only partly met in some cases. The model both over and under-estimated measured sublimation rates but generally captured the magnitude and timing of sublimation events. The modelled results do not display the sharp diurnal cycling of the measured values, possibly because the model does not include a term for conductive heat flux between snow and branches. As the sublimation model does not include snow interception in this run the model develops substantial errors where small snowfalls occur during the sublimation event; examples are bursts of apparent "negative sublimation" on Days 61 and 79 of 1995 (Fig 5b, c). Between days 74 and 79 in 1996 the model underestimated the measured "sublimation" (Fig. 5f, g), however the rapid mass loss from the suspended tree in this period may have had additional contributions from unloading or melt, as indicated by the high peak air temperatures during the period or the model may have underestimated radiant energy inputs to sublimation as these events received average net radiation 2.5 to 4 times higher than the others modelled (Table 1).

Table 1. Meteorological conditions during sublimation events measured and modelled in 1995 and 1996.

Event	Julian Day / year	Mean $T_a$	Max $T_a$	Min $T_a$	Mean U	Peak U	Mean RH	Min RH	Mean $Q^*$
A	40-50 /95	-21.4	-9.2	-35.6	2.8	6.8	65	42	28
B	57-65 /95	-21.7	-3.9	-36.3	2	4.4	63	33	38
C	76- 81 /95	-3	4.5	-10.8	2.4	6.9	79	47	27
D	45-47 /96	-12.1	-2.8	-27.1	2.8	6.3	69	40	29
E	50-54 /96	-7.2	4.7	-22.9	2.8	4.8	80	46	37
F	74 /96	0	7.2	-6.7	3.1	5.4	66	31	102
G	76-78 /96	-8.3	-0.2	-15.4	1.7	4.2	77	42	91

$T_a$  is ambient air temperature in the canopy ( $^{\circ}\text{C}$ ), RH is relative humidity in the canopy (%), U is wind speed 8 m above the canopy ( $\text{m s}^{-1}$ ) and  $Q^*$  is net radiation above the canopy ( $\text{W m}^{-2} \text{s}^{-1}$ ). Maximum and minimum values are for half-hour periods.



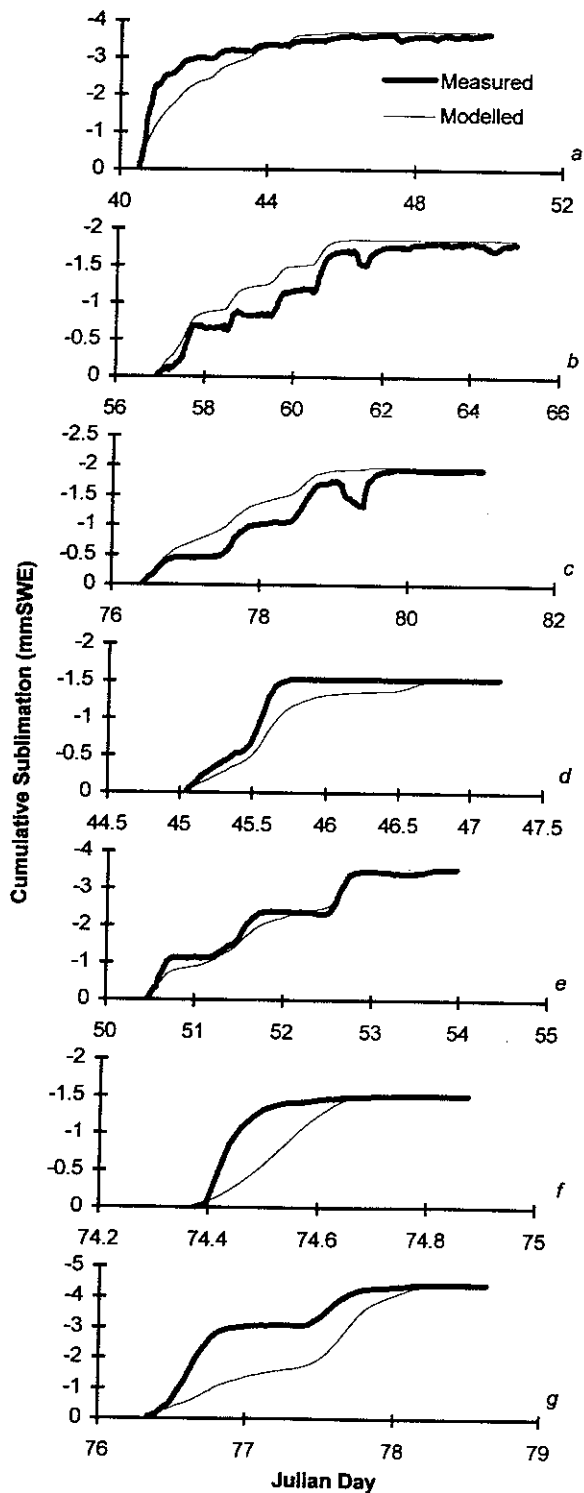


Figure 5. Cumulative sublimation measured using loss of snow mass on a weighed pine tree and modelled using the sublimation equations and a measured initial snow load for the seven sublimation events described in Table 1.

To evaluate the daily performance of the model, the daily modelled and measured sublimation fluxes are graphed in Fig. 6 for all events. Such a daily comparison will tend to reduce the effect of storage terms such as canopy heat storage and subsequent flux to or from intercepted snow. There is a reasonable correspondence between modelled and measured daily results for smaller sublimation fluxes with increasing scatter for the largest events. Two large sublimation days ( $> 2.5 \text{ mm SWE d}^{-1}$ ) were underestimated by the model by 60%-70%, as noted above the causes may be underestimate of radiant energy input in the model or to unloading/melt counted as sublimation in the "measured" value. One large sublimation day ( $> 1.4 \text{ mm SWE d}^{-1}$ ) was overestimated two-fold by the model. The mean daily error in sublimation estimate (measured - modelled) is  $-0.027 \text{ mm SWE d}^{-1}$  with a standard deviation of error equal to  $0.448 \text{ mm SWE}$ , suggesting that the model produces reasonable average sublimation losses.

Many applications (GCMs, mesoscale atmospheric models) require information on how long the canopy is subject to enhanced latent heat fluxes. To test this estimation by the sublimation routine, the modelled time to complete sublimation was compared to the length of time that the weighed tree retained a snow load for each event. As shown in Fig. 7, the sublimation model slightly overestimated the time required to complete sublimation. The mean error (measured - modelled) in estimated time to complete sublimation was  $-11.3 \text{ hours}$  with a standard deviation of  $13.6 \text{ hours}$ . The cumulative error over all seven periods was a 7.3% overestimate of snow-covered time. It is expected that some of the difference is due

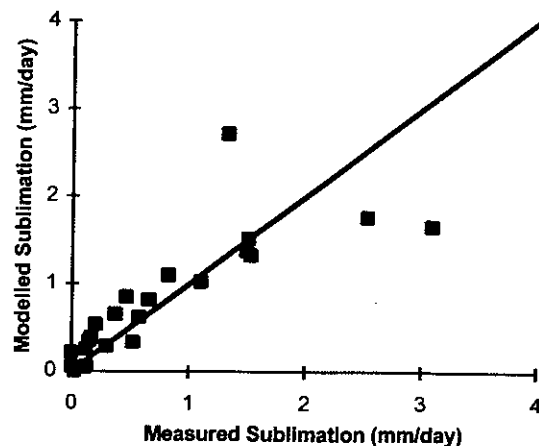


Figure 6. Daily measured sublimation fluxes, calculated from the loss of snow mass from a weighed pine tree versus modelled sublimation, calculated from a measured initial snow load and the sublimation equations.

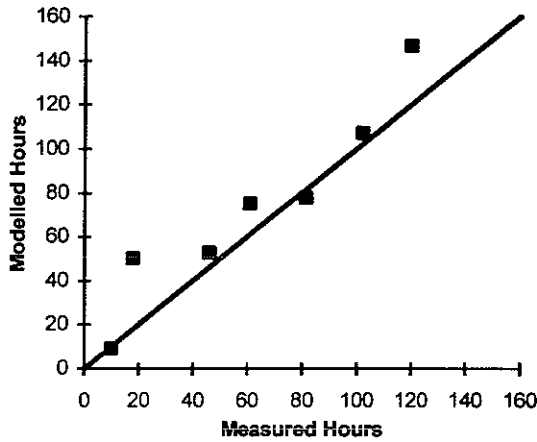


Figure 7. Time required to complete sublimation, measured and modelled sublimation calculated as for Fig. 6 until measured intercepted snow was depleted.

to unloading, which was not calculated in this test but is included in the coupled runs shown in the next section.

#### Coupled Interception-Sublimation Model

The coupled interception-sublimation model uses the interception equations on a half hourly basis to estimate intercepted snow load and then calculates sublimation and unloading loss (ablation). The final snow load from each iteration is used for the subsequent calculation, the procedure repeated throughout the snowfall-sublimation sequence. The analysis for the seven sublimation sequences is expanded now to include the preceding snowfall period. Figure 8 shows the result of modelled and measured interception-ablation sequences, expressed as intercepted snow load (mm SWE). The pattern of modelled sequences of intercepted snow load accumulation and ablation match much of the measured sequence, with the exception of Days 45 & 50 1996 (Fig. 8d, e) when interception was underestimated. A comparison of half-hourly modelled and measured snow loads is shown in Fig. 9 and shows consistent over or underestimates over the course of each event with the exception of Fig. 9g where snow load was underestimated during the accumulation period and overestimated during ablation. For the suite of events, a mean error (measured - modelled) of 0.062 mm SWE with a standard deviation of 0.46 mm SWE suggests relatively good composite performance.

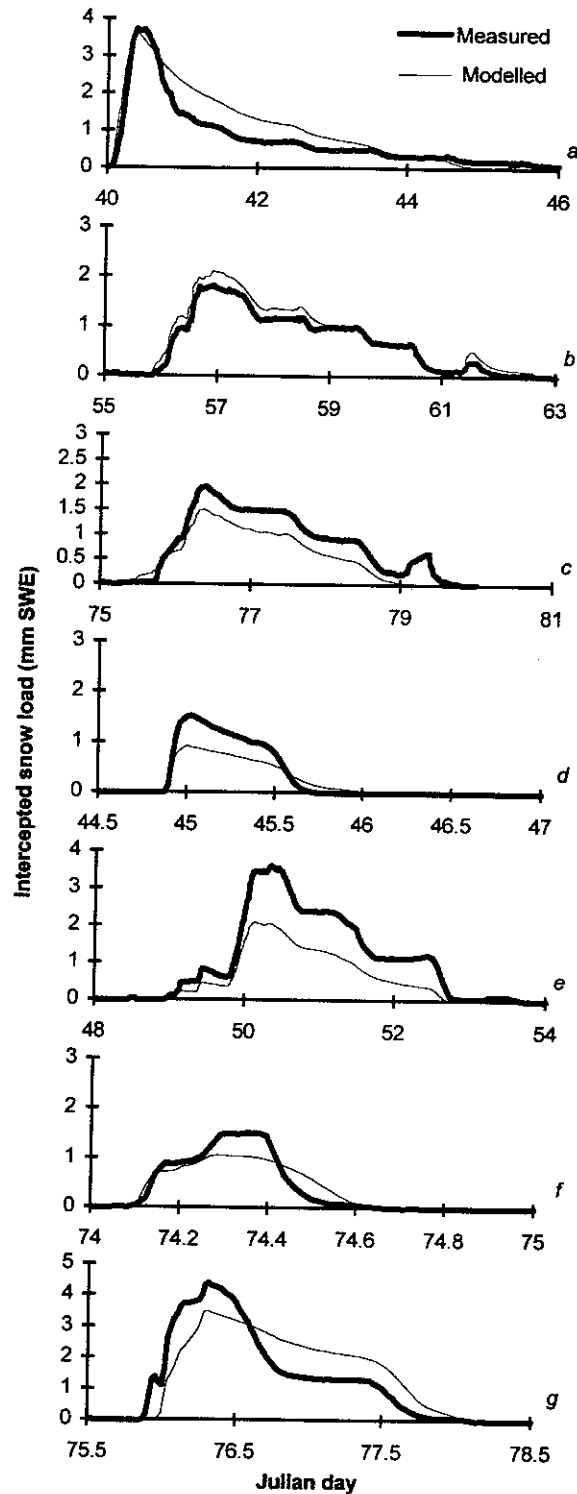


Figure 8. Sequences of measured intercepted snow load, calculated from the mass of snow on a suspended tree, and estimated intercepted snow load modelled using the coupled snow interception-sublimation model. Conditions for interception and sublimation are described in Tables 1 and 2.

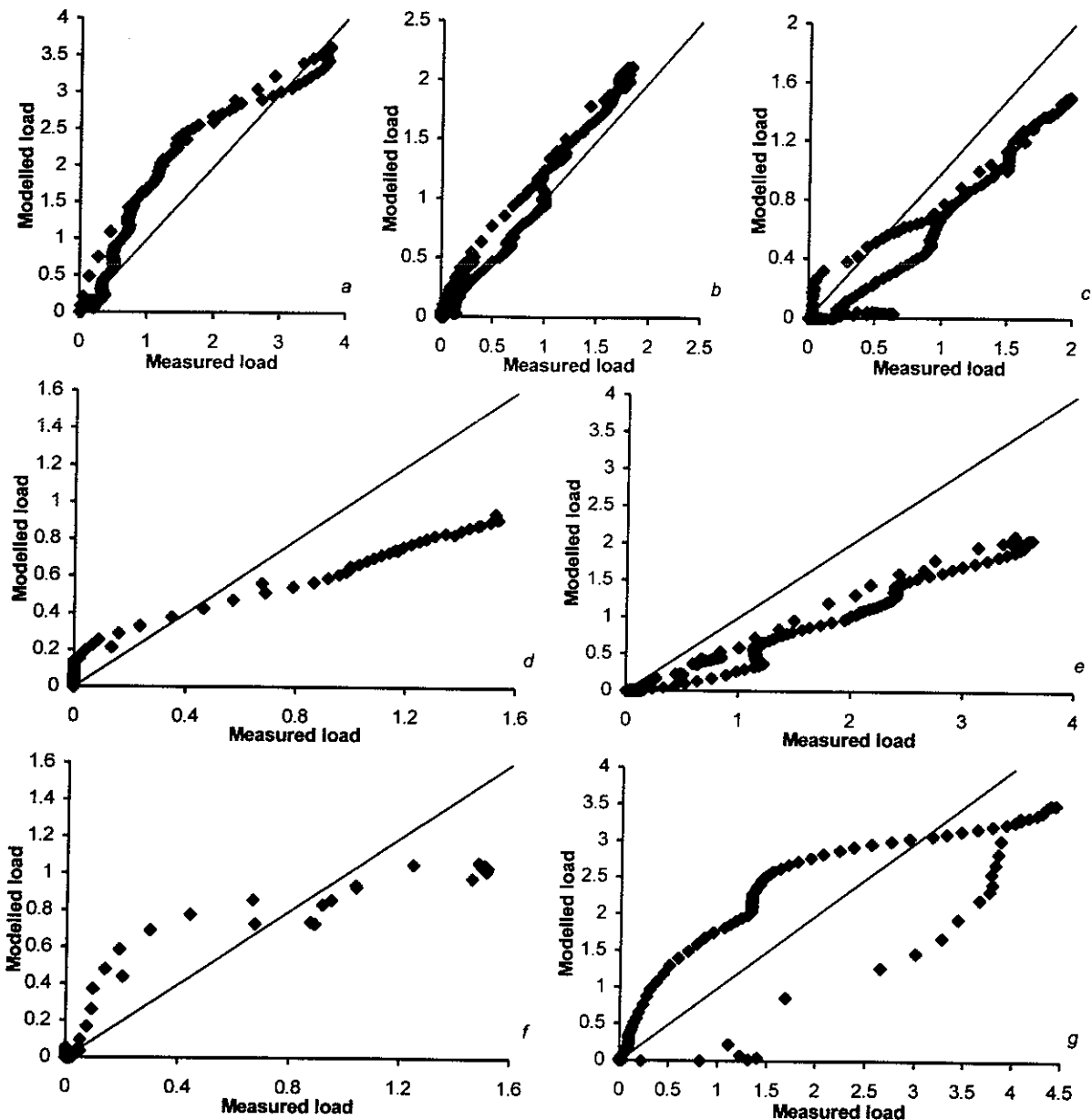


Figure 9. Comparison of half-hourly calculated measured and modelled intercepted snow loads as determined for Fig. 8. Conditions for interception and sublimation are described in Tables 1 and 2.

#### Modelled Events in an Annual Context

The modelled events form only part of the annual sequence of snow interception and ablation. To summarize the modelled events, Table 2 shows the snowfall, interception, sublimation and length of time with snow-covered canopy for each of the seven events. Modelled interception efficiency (before unloading) ranged from 85% to 95%, whilst modelled sublimation consumed from 58% to 65% of snowfall over the period, the difference between interception and sublimation loss is due to unloading. Measured sublimation losses over the events considered were 9.3 and 11.7 mm SWE for 1995 and 1996,

respectively, with corresponding snowfall over the events of 17 and 15 mm SWE. This suggests that sublimation actually consumed from 55% to 78% of snowfall over the period. The model overestimated the snow-covered period by 7.0 hours per event.

To examine the seasonal and forest-wide context of the model runs, weekly corrected sub-canopy snowfall measurements were subtracted from above-canopy measurements providing estimates of weekly snow interception for the 1994-95 and 1995-96 seasons in three canopies: jack pine, mixed wood (white spruce/ trembling aspen) and black spruce. By the end of the season when the canopy snow load is

**Table 2. Snowfall, interception, intercepted snow load, sublimation and snow-covered time for the seven events as measured and modelled using the coupled interception-sublimation model.**

Event	Snowfall (mm SWE)	Modelled interception (mm SWE)	Peak load, measured (mm SWE)	Modelled sublimation (mm SWE)	Measured sublimation (mm SWE)	Length of time snowcovered (hours)	
						Measured	Modelled
A	7.3	6.2	3.7	4.2	4.0	129.0	154.5
B	6.1	5.6	2.6	3.9	2.8	166.0	174.0
C	3.6	3.4	2.0	2.3	2.5	110.0	104.5
D	1.9	1.8	1.5	1.2	1.5	20.5	45.0
E	4.3	4.0	3.6	2.7	4.0	122.0	111.5
F	2.0	1.9	1.5	1.3	1.5	16.0	19.0
G	6.8	5.8	4.4	4.0	4.7	56.0	60.0

zero, any difference between above and sub-canopy snowfall is due to sublimation of intercepted snow as the environment is cold and dry (see Table 1). Figure 10 shows weekly snow interception (*not* snow load) from November through April of each season, expressed as a percentage of cumulative seasonal snowfall to that date. It is seen that substantial portions of snowfall are intercepted early in the winter, with the greatest interception in the dense spruce canopy (up to 67% of cumulative snowfall in late November 1994) and the lowest in the mixed-wood canopy (only 9% in February, 1995). The pine canopy interception is between the others, ranging from 44% in December

1994 to 30% by April 1995. The lower snowfall winter of 1995-96 (97 mm SWE) had a smaller range of interception/snowfall percentages than did the higher snowfall season of 1994-95 (122 mm SWE).

The percentage of snowfall intercepted at the end of winter is equivalent to the seasonal sublimation loss, which for the pine ranged from 30% to 32% or 39 and 29 mm SWE in 1994-95 and 1995-96, respectively. Hence the sublimation modelled from Day 40-80 of each year contributed to 24% in 1995 and 40% in 1996 of seasonal sublimation, reasonable values for the length of time (40 days) compared to the winter season length (approx 150 days) and considering that the period occurred in late winter when temperatures are warmer than the season average. Seasonal sublimation losses amongst stand types, showed the pine to be between values for the black spruce (38%-45% of seasonal snowfall) and mixed-wood (10%-15% of seasonal snowfall). The seasonal and stand results suggest that the modelled sublimation quantities are reasonable and mid-way between those found in various stands of the southern boreal forest. The evaluation period however, reflects times with high interception efficiency and hence sublimation loss per unit of snowfall than the seasonal average.

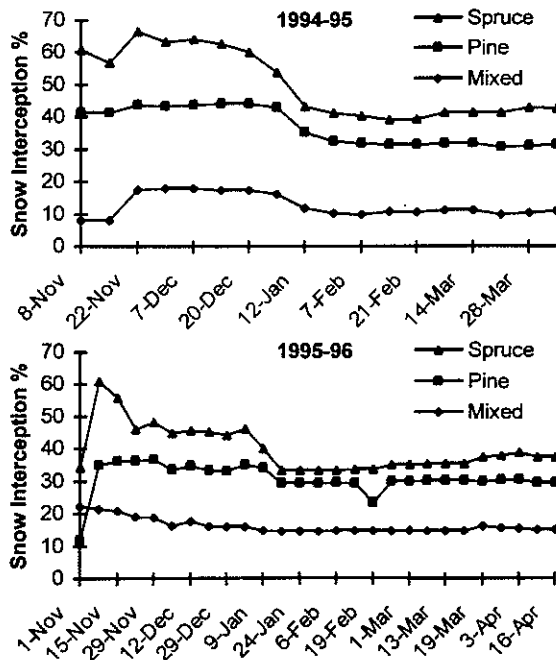


*Figure 10. Snow interception as a percentage of cumulative snowfall over two seasons for three mature stands (black spruce, jack pine, mixed white spruce/trembling aspen) in the southern boreal forest near Waskesiu Lake, Saskatchewan. Interception is estimated as above-canopy - sub-canopy snowfall.*

**CONCLUSIONS**

A process-based coupled snow interception-sublimation model has been developed by scaling the processes of turbulent heat and mass transfer from snow crystal to canopy scale and scaling the processes of snow loading and unloading from branch to canopy scale. Scaling is accomplished using fractal mathematics and scaling parameters based on leaf area of the stand. The model uses snowfall, incoming solar radiation, within-canopy wind speed, air temperature and humidity, and forest stand mensuration descriptors to calculate snow interception and sublimation for short-time iterations. Intercepted snow load, calculated as interception - sublimation -

unloading, is used to determine snow interception efficiency in the subsequent iteration.

Tests in late winter in a southern boreal forest jack pine stand against measured interception and sublimation, estimated using the mass of snow and rate of change in mass on a weighed full-size pine, found the model provides reasonable approximations of both interception and sublimation losses on half-hourly, daily and event basis. Cumulative errors in estimating intercepted snow load over 23 days of test were 0.06 mm SWE. Sublimation was rapid in the test period, up to 3 mm/day and consuming approximately two-thirds of snowfall during the period. Seasonal intercepted snow sublimation as a portion of annual snowfall at the model test site was lower than losses measured during the tests, ranging from 13% for a mixed spruce-aspens, 31% for the mature pine and 40% for a mature spruce stand. This indicates that seasonal sublimation losses are substantial, but late-winter sublimation is particularly important. Further evaluation of the model throughout a season and in other environments is warranted as is a more detailed examination of the unloading process and role of radiation to intercepted snow in driving sublimation.

#### ACKNOWLEDGEMENTS

The authors acknowledge the assistance and guidance of Dr. R.A. Schmidt, US Forest Service and Dr. R. Harding, Institute of Hydrology (UK) in various stages of this study. Funding was provided by the Canadian GEWEX Programme; Prince Albert Model Forest Association; Prince Albert National Park; National Hydrology Research Institute; Climate Research Network and the Natural Sciences and Engineering Research Council of Canada. Field work was assisted by Cuyler Onclin, Kelly Best, Tom Carter, John Mollison, Ken Dion and Karla Foster of the National Hydrology Research Institute and Dell Bayne and Ed Cey of the Division of Hydrology, University of Saskatchewan.

#### REFERENCES

- Barry, P.J. 1991. Discussion paper on the report by H.G. Jones entitled "Snow chemistry and biological activity: a particular perspective on nutrient cycling". In, (eds. T.D. Davies, M. Tranter and H.G. Jones) *Seasonal Snowpacks: Processes of Compositional Change*. NATO ASI Series G(28). Springer-Verlag, Berlin. 229-235.
- Brown, T. and J.W. Pomeroy. 1989. A blowing snow particle detector. *Cold Regions Science and Technology*, 16. 167-174.
- Brundl, M., Schneebli, M. and H. Flüeler. 1997. Snow interception in a spruce crown in different weather conditions. *Journal of Hydrology* (in press).
- Claasen, H.C. and J.S. Downey. 1995. A model for deuterium and oxygen 18 isotope changes during evergreen interception of snowfall. *Water Resources Research*, 31. 601-618.
- Essery, R. 1998. Boreal forests and snow in climate models. *Hydrological Processes*. In press.
- Gower S.T. and J.M. Norman. 1991. Rapid estimation of leaf area index in conifer and broad-leaf plantations. *Ecology*, 72(5). 1896-1900.
- Harding, R.J. and J.W. Pomeroy. 1996. The energy balance of the winter boreal landscape. *Journal of Climate*, 9. 2778-2787.
- Hedstrom, N.R. and J.W. Pomeroy. 1998. Accumulation of intercepted snow in the boreal forest: measurements and modelling. *Hydrological Processes*, in press.
- Kuz'min, P.P. 1963. *Formirovanie Snezhnogo Pokrova i Metody Opredeleniya Snegozapasov* (Snow Cover and Snow Reserves). [English translation by Israel Program for Scientific Translation, Jerusalem]. 139 p.
- Lee, L.W. 1975. Sublimation of snow in a turbulent atmosphere. PhD Thesis. University of Wyoming, Laramie, USA. 162 p.
- Lundberg, A. and S. Halldin. 1994. Evaporation of intercepted snow - an analysis of governing factors. *Water Resources Research*, 30: 2587-2598.
- Lundberg, A. and S. Halldin (in press) Snow interception evaporation: review of rates, processes, models and measurement techniques. *Agricultural and Forest Meteorology*, submitted.
- Lundberg, A., I. Calder and R. Harding. 1998. Evaporation of intercepted snow: measurements and modelling. *Journal of Hydrology*. In press.
- Mandelbrot, B.B. 1983. *The Fractal Geometry of Nature*. W.H. Freeman and Company, NY, NY. 468 p.
- McNay, R.S., Petersen, L.D. and J.B. Nyberg. 1988. The influence of forest stand characteristics on snow interception in the coastal forests of British Columbia. *Canadian Journal of Forest Research*, 18. 566-573.

- Miner, N.H. and J.M. Trappe. 1957. *Snow Interception, Accumulation and Melt in Lodgepole Pine Forests in the Blue Mountains of Eastern Oregon*. USDA Forest Research Service, Forest and Range Experimental Station, Research Note No. 143. 4 p.
- Nakai, Y., Kitahara, H., Sakamoto, T., Saito, T. and T. Terajima. 1993. Evaporation of snow intercepted by forest canopies. *Journal of the Japanese Forestry Society*, 75. 191-200 (in Japanese, English summary)
- Nakai, Y., Sakamoto, T., Terajima, T., Kitahara, H. and T. Saito. 1994. Snow interception by forest canopies: weighing a conifer tree with meteorological observation and analysis with Penman-Monteith formula. *IAHS Publication No. 223*. IAHS Press, Wallingford, UK. 227-236.
- Nakai, Y., Sakamoto, T., Terajima, T., Kitamura, K. and T. Shirai. (in press) Energy balance above a boreal coniferous forest: a difference in turbulent fluxes between snow-covered and snow-free canopies. *Hydrological Processes*. In press.
- Pomeroy, J.W. 1989. A process-based model of snow drifting. *Annals of Glaciology*, 13. 237-240.
- Pomeroy, J.W. and R.A. Schmidt. 1993. The use of fractal geometry in modelling intercepted snow accumulation and sublimation. *Proceedings of the 50th Annual Eastern Snow Conference*. 1-10.
- Pomeroy, J.W. and D.M. Gray. 1995. *Snowcover Accumulation, Relocation and Management*. NHRI Science Report No. 7. National Hydrology Research Institute, Environment Canada, Saskatoon, SK. 134 p.
- Pomeroy, J.W. and K. Dion, 1996. Winter radiation extinction and reflection in a boreal pine canopy: measurements and modelling. *Hydrological Processes*, 10. 1591-1608.
- Pomeroy, J.W., D.M. Gray and P.G. Landine (1993) "The Prairie Blowing Snow Model: characteristics, validation, operation" *Journal of Hydrology*, 144. 165-192.
- Pomeroy, J.W., R.J. Granger, A. Pietroniro, J. Elliott, B. Toth and N. Hedstrom. 1997. *Hydrological Pathways in the Prince Albert Model Forest*. NHRI Contribution Series No. CS-97004. Saskatoon, National Hydrology Research Institute. 154 p.
- Pomeroy, J.W., D.M. Gray, K.R. Shook, B. Toth, R.L.H. Essery, A. Pietroniro, and N. Hedstrom. 1998. An evaluation of snow processes for land surface modelling. *Hydrological Processes*. In press.
- Schmidt, R.A. 1972. Sublimation of wind-transported snow: a model. *USDA Forest Service Research Paper RM-90*. Fort Collins, Rocky Mountain Forest and Range Experiment Station. 24 p.
- Schmidt, R. A. 1991. Sublimation of snow intercepted by an artificial conifer; *Agricultural and Forest Meteorology*, 54. 1-27
- Schmidt, R.A. and D.R. Gluns. 1991. 'Snowfall interception on branches of three conifer species', *Canadian Journal of Forest Research*, 21. 1262-1269.
- Schmidt, R.A., R.L. Jairell and J.W. Pomeroy. 1988. Measuring snow interception and loss from an artificial conifer, *Proceedings of the Western Snow Conference*, 56. 166-169.
- Shook, K., D.M. Gray and J.W. Pomeroy. 1993. Temporal variations in snowcover area during melt in Prairie and Alpine environments. *Nordic Hydrology*, 24. 183-198.
- Swanson, R.H. 1988. The effect of *in situ* evaporation on perceived snow distribution in partially clear-cut forests. *Proceedings of the Western Snow Conference*, 56. 87-92.
- Taylor, C.M., Harding, R.J., Pielke, R.A., Pomeroy, J.W., Vidale, P.L. and R.L. Walko (1998) Snow breezes in the boreal forest. *Journal of Geophysical Research*. In press.
- Thorpe, A. and B. Mason. 1966. The evaporation of ice spheres and crystals. *British Journal of Applied Physics*, 17. 541-548
- Toews, D.A. and D.R. Gluns. 1986. Snow accumulation and ablation on adjacent forested and clearcut sites in southeastern British Columbia. *Proceedings of the Western Snow Conference*, 54. 101-111.
- Troendle, C.A. and J.R. Meiman. 1984. Options for harvesting timber to control snowpack. *Proceedings of the Western Snow Conference*, 52. 86-98.
- Wilm, H.G. and E.F. Dunford. 1945. *Effect of Timber Cutting on Water Available for Streamflow from a Lodgepole Pine Forest*. USDA Technical Bulletin No. 965. 43 p.